GEOMETRICAL SCALING IN HADRONIC COLLISIONS*

Michal Praszalowicz

The Marian Smoluchowski Institute of Physics, Jagiellonian University
Reymonta 4, 30-059 Krakow, Poland
michal@if.uj.edu.pl

(Received April 29, 2011)

We show that the p_{T} spectra measured in pp collisions at the LHC exhibit geometrical scaling introduced earlier in the context of deep inelastic scattering. We also argue that the onset of geometrical scaling can be seen in nucleus–nucleus collisions at lower RHIC energies.

DOI:10.5506/APhysPolB.42.1557
PACS numbers: 13.85.–t, 11.80.Fv

1. Introduction

With the start of the LHC we have been confronted with a wealth of data on multiparticle production at high energies both in pp [1,2,3] and in heavy ion collisions [4]. One of the remarkable results is that total multiplicity of charged particles produced in central rapidity in pp collisions is rising like a power of s

$$\frac{dN_{\mathrm{ch}}}{d\eta} \sim s^{\tilde{\lambda}} \quad \text{with} \quad \tilde{\lambda} \simeq 0.23\,. \tag{1}$$

The power law behavior (1) is expected in saturation models [5, 6, 7, 8, 9, 10]. In this paper we show that power like behavior of total multiplicity follows naturally if p_{T} spectra of charged particles exhibit geometrical scaling [11, 12]. In Sec. 2 we remind basic properties of geometrical scaling which was introduced in the context of small x deep inelastic scattering (DIS). In Sec. 3 we introduce geometrical scaling in pp collisions. In Sec. 4 we briefly discuss a possibility of geometrical scaling in heavy ion collisions. Finally, we summarize and give conclusions in Sec. 5.

* Based on a talk presented at the Cracow Epiphany Conference on the First Year of the LHC, Cracow, Poland, January 10–12, 2011.

2. Geometrical scaling in DIS

In a successful description of small x DIS proposed in seminal papers by Golec-Biernat and Wüsthoff (GBW model) [13], a cross-section for virtual photon–proton scattering in DIS reads

$$\sigma_{\gamma^* p} = \int dr^2 \left|\psi(r,Q^2)\right|^2 \sigma_{dP}(r^2 Q_{\rm s}^2(x)). \tag{2}$$

Here ψ is the wave function describing dissociation of a virtual photon into a $q\bar{q}$ dipole and σ_{dP} is a dipole-proton cross-section. The main assumption of the GBW model is that σ_{dP} which in principle is a function of two independent variables: dipole size r and dipole-proton energy W (or Bjorken x), depends in practice only on a certain combination of these two variables, namely on the product $r^2 Q_{\rm s}^2(x)$, where

$$Q_{\rm s}^2(x) = Q_0^2 \left(\frac{x_0}{x}\right)^{\lambda} \tag{3}$$

is called a saturation scale. Bjorken x is defined as

$$x = \frac{Q^2}{Q^2 + W^2}\,. \tag{4}$$

Here $Q_0 \sim 1$ GeV and $x_0 \sim 10^{-3}$ are free parameters whose precise values can be extracted by fitting (2) to the HERA data. Power λ is known to be of the order of $\lambda \sim 0.2 \div 0.3$.

For transverse photons (neglecting quark masses)

$$\left|\psi_{\rm T}\left(r,Q^2\right)\right|^2 = \int\limits_0^1 dz \left[z^2 + (1-z)^2\right] \overline{Q}^2 K_1^2\left(\overline{Q}r\right)\,, \tag{5}$$

where

$$\overline{Q}^2 = z(1-z)Q^2 \tag{6}$$

and K_1 is a modified Bessel function. From Eq. (5) it follows that

$$\left|\psi_{\rm T}\left(r,Q^2\right)\right|^2 = Q^2 \left|\tilde{\psi}_{\rm T}(rQ)\right|^2\,, \tag{7}$$

where we have explicitly factored out Q^2. Defining new variable $u = Q^2 r^2$, new function $\phi(u) = u|\tilde{\psi}_{\rm T}(u)|^2$ and *scaling variable* τ

$$\tau = \frac{Q^2}{Q_{\rm s}^2(x)} \tag{8}$$

we arrive at

$$\sigma_{\gamma^* p} = \int \frac{du}{u}\phi(u)\sigma_{dP}(u\tau)\,. \tag{9}$$

It follows that $\sigma_{\gamma^* p}$ is a function of scaling variable τ, rather than a function of two variables Q^2 and x. This phenomenon is known as geometrical scaling (GS) [14]. GS has been observed in DIS data for $x < 0.01$.

In the Golec-Biernat–Wüsthoff model

$$\sigma_{dP}\left(r^2 Q_{\mathrm{s}}^2(x)\right) = \sigma_0\left(1 - \exp\left(-r^2 Q_{\mathrm{s}}^2(x)\right)\right)\,, \tag{10}$$

where σ_0 is dimensional constant; $\sigma_0 \simeq 23$ mb.

In practice, Q_{s}^2 may also have some residual dependence on Q^2 if DGLAP evolution in (2) is taken into account [15]. Indeed, it can be shown that in the GBW model — up to logarithmic corrections — DIS structure function is proportional to Q_{s}^2

$$\sigma_{\gamma^* p}\left(x, Q^2\right) \sim \sigma_0 \frac{Q_{\mathrm{s}}^2(x)}{Q^2} \quad \text{and} \quad F_2\left(x, Q^2\right) \sim \sigma_0 Q_{\mathrm{s}}^2(x)\,. \tag{11}$$

At first sight Eq. (11) may look contradictory, since left-hand sides depend non-trivially on Q^2 and the right-hand sides do not. In practice, exact calculation of the integral in (2) renders some mild Q^2 dependence of the right-hand sides. Moreover, DGLAP evolution introduces Q^2 dependence of $Q_{\mathrm{s}}^2(x)$. Therefore, the effective saturation scale can be conveniently parameterized as

$$Q_{\mathrm{s,eff}}^2\left(x, Q^2\right) = Q_0^2\left(\frac{x_0}{x}\right)^{\lambda_{\mathrm{eff}}\left(Q^2\right)}\,. \tag{12}$$

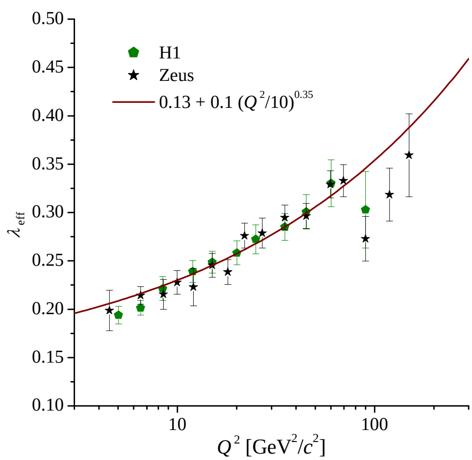

Fig. 1. Dependence of λ_{eff} on Q^2 from HERA (HERA data points [16] after Ref. [17]).

Exponent $\lambda_{\rm eff}(Q^2)$ has been extracted from the HERA data [16]. This is shown in Fig. 1 (after Ref. [17]) together with an eyeballing fit [12]

$$\lambda_{\rm eff}(Q) = 0.13 + 0.1\left(\frac{Q^2}{10}\right)^{0.35} . \tag{13}$$

3. Geometrical scaling in *pp* collisions

In pp collisions we do not have a viable model of low and medium $p_{\rm T}$ particle production at high energies. Nevertheless one often uses a $k_{\rm T}$ factorized form of a cross-section describing production of a $p_{\rm T}$ gluon at rapidity y [18]

$$E\frac{d\sigma}{d^3p} = \frac{3\pi}{2}\frac{1}{p_{\rm T}^2}\int dk_{\rm T}^2 \alpha_{\rm s}(k_{\rm T})\varphi_1\left(x_1,k_{\rm T}^2\right)\varphi_2\left(x_2,(k-p)_{\rm T}^2\right) , \tag{14}$$

where

$$x_{1,2} = \frac{p_{\rm T}}{\sqrt{s}}e^{\pm y} \tag{15}$$

are Bjorken xs of colliding partons. Here φs are unintegrated gluon densities. Introducing "regular" gluon distribution

$$xG\left(x,Q^2\right) = \int^{Q^2} dk_{\rm T}^2\varphi\left(x,k_{\rm T}^2\right) \tag{16}$$

one obtains for $p_{\rm T}^2 > Q_{\rm s}^2$

$$E\frac{d\sigma}{d^3p} = \frac{3\pi}{2}\frac{\alpha_{\rm s}(Q_{\rm s})}{p_{\rm T}^2}\left\{\varphi_1\left(x_1,p_{\rm T}^2\right)x_2G\left(x_2,p_{\rm T}^2\right) + \varphi_2\left(x_2,p_{\rm T}^2\right)x_1G\left(x_1,p_{\rm T}^2\right)\right\} . \tag{17}$$

There have been recently more involved model calculations of particle multiplicity based on Eq. (14) [19, 20, 21].

Kharzeev an Levin proposed a simple Ansatz for unintegrated gluon distribution [22]

$$\varphi\left(x,p_{\rm T}^2\right) = \frac{3\sigma_0}{\pi^2\alpha_{\rm s}\left(Q_{\rm s}^2\right)}\left\{\begin{array}{ccc} 1 & \text{for} & p_{\rm T}^2 < Q_{\rm s}^2 , \\ Q_{\rm s}^2/p_{\rm T}^2 & \text{for} & Q_{\rm s}^2 < p_{\rm T}^2 . \end{array}\right. \tag{18}$$

Hence, up to the logarithmic corrections due to the running coupling constant, we arrive at geometrical scaling for the multiplicity distribution

$$\frac{dN_{\rm ch}}{d\eta d^2p_{\rm T}} = \frac{1}{\sigma_{\rm inel}}E\frac{d\sigma}{d^3p} = \frac{1}{Q_0^2}F(\tau) , \tag{19}$$

where $Q_0 \sim 1$ GeV and $\sigma_{\rm inel}$ is the inelastic cross-section. Although we have used a very simple Ansatz (18) for unintegrated gluon distribution φ, it satisfies the generic property that $xG(x, Q_s^2) \sim Q_s^2$ which is enough for GS to hold.

$F(\tau)$ is a universal function of the scaling variable

$$\tau = \frac{p_{\rm T}^2}{Q_{\rm s}^2}\,, \tag{20}$$

where in view of (3) and (15)

$$Q_{\rm s}^2 = Q_0^2 \left(\frac{p_{\rm T}}{W}\right)^{-\lambda}\,, \tag{21}$$

where $W = \sqrt{s} \times 10^{-3}$. Here factor 10^{-3} corresponds to the (arbitrary at this moment) choice of x_0.

The power like growth of the multiplicity can be easily understood as a consequence of geometrical scaling. Indeed

$$\frac{dN_{\rm ch}}{dy} = \int \frac{dp_{\rm T}^2}{Q_0^2} F(\tau)\,. \tag{22}$$

Simple change of variables gives [11]

$$\frac{dp_{\rm T}^2}{Q_0^2} = \frac{2}{2+\lambda}\left(\frac{W}{Q_0}\right)^{\frac{2\lambda}{2+\lambda}} \tau^{-\frac{\lambda}{2+\lambda}} d\tau\,. \tag{23}$$

The integral over $d\tau$ is convergent and *universal*, *i.e.* it does not depend on energy. It follows from Eq. (23) that the effective power of the multiplicity growth is

$$\tilde{\lambda} = \frac{2\lambda}{2+\lambda} < \lambda \tag{24}$$

rather than λ. For $\lambda = 0.27$ we have that $\tilde{\lambda} = 0.238$.

In Refs. [11] it was shown that CMS charged particle $p_{\rm T}$ spectra [2] at mid rapidity $|\eta| < 2.4$ plotted as functions of scaling variable τ fall on one universal curve (19). This is depicted in Fig. 2, where we plot $p_{\rm T}$ spectra for three LHC energies as functions of $p_{\rm T}^2$ (left panel) and as functions of scaling variable τ for $\lambda = 0.27$ (right panel).

In order to examine the quality of geometrical scaling in *pp* collisions we plot in Fig. 3 ratios of spectra measured at 7 TeV to spectra at 0.9 and 2.36 TeV in function of $p_{\rm T}$ (left panel) and $\sqrt{\tau}$ (right panel). We see that original ratios plotted in terms of $p_{\rm T}$ range from 1.5 to 7, whereas plotted in terms of $\sqrt{\tau}$ they are well concentrated around unity. This is further illustrated in

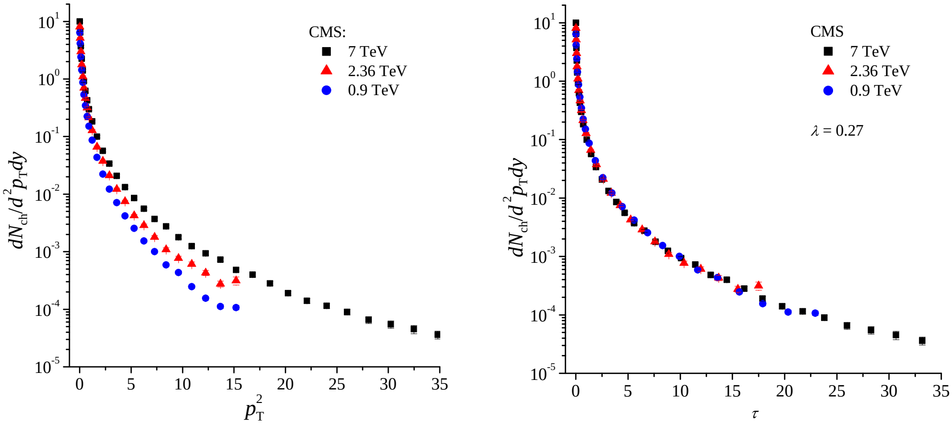

Fig. 2. Charged particle multiplicity at mid rapidity $|\eta| < 2.4$ as measured by CMS [2], plotted as functions of p_T^2 (left) and scaling variable τ (right) for $\lambda = 0.27$.

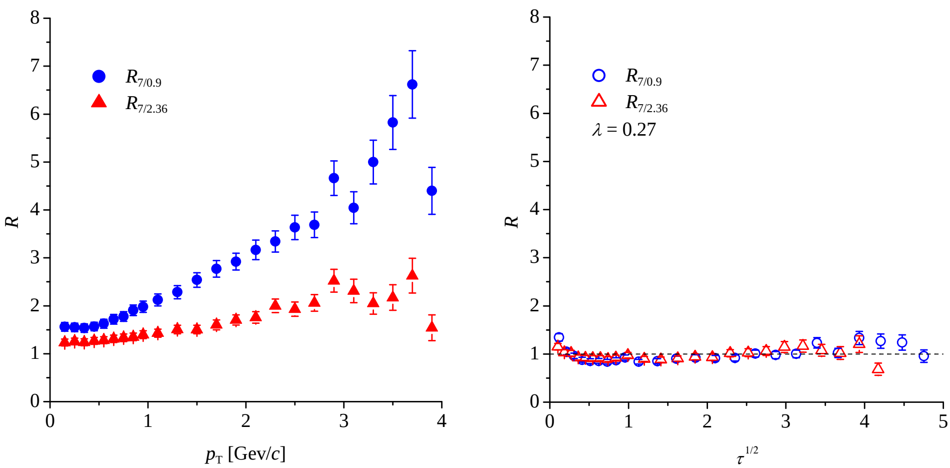

Fig. 3. Ratios of CMS p_T spectra [2] at 0.7 TeV to 0.9 (blue circles) and 2.36 TeV (red triangles) plotted as functions of p_T (left) and scaling variable $\sqrt{\tau}$ (right) for $\lambda = 0.27$.

the left panel of Fig. 4 which presents the enlarged view of the right panel of Fig. 3. With this accuracy we see a small systematic increase of the ratios (apart from the first 4, 5 points which correspond to particles of very low p_T where a different production mechanism may dominate) which suggests some weak dependence of exponent λ on p_T. The value of $\lambda = 0.27$ has been obtained by minimizing deviations of ratios $R_{7/0.9}$ and $R_{7/2.36}$ from 1 for central p_T points (*i.e.* rejecting first 5 and last 4 points).

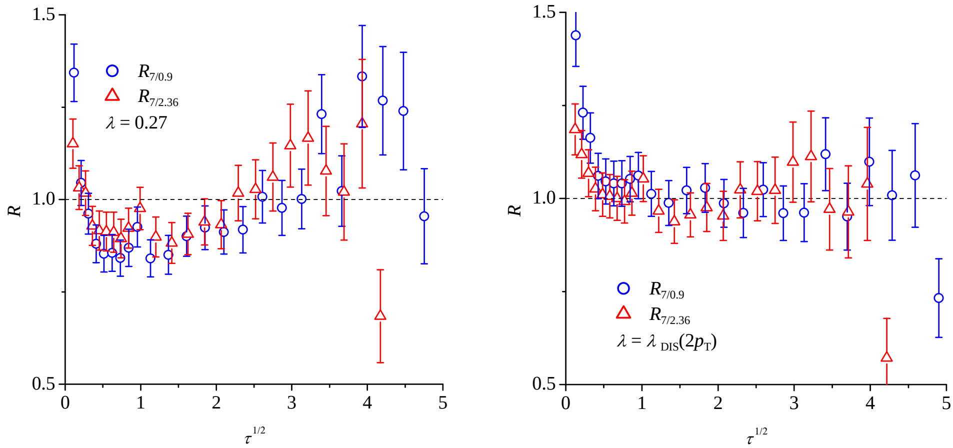

Fig. 4. Enlarged plot of the right panel of Fig. 3 for $\lambda = 0.27$ (left) and for $\lambda = \lambda_{\rm eff}(2p_{\rm T})$.

Residual dependence of exponent λ on $p_{\rm T}$ is in agreement with small x dependence of the DIS structure function as measured in HERA [16]. In Ref. [12] we have argued that this dependence can be well approximated by use of the effective exponent $\lambda_{\rm eff}$ of Eq. (13) with argument $Q = 2p_{\rm T}$. This is demonstrated in the right panel of Fig. 4, where we used $\lambda_{\rm eff}(2p_{\rm T})$ to calculate the ratios $R_{7/0.9}$ and $R_{7/2.36}$. An impressive improvement of geometrical scaling (*i.e.* of the equalities $R_{7/0.9} \simeq 1$ and $R_{7/2.36} \simeq 1$) can be indeed seen.

4. Onset of geometrical scaling in heavy ion collisions

Heavy ions provide much reacher information on the characteristics of particle production at high energies. Indeed, one can study not only energy dependence but also atomic number A-dependence, rapidity dependence (at RHIC much larger rapidity range has been covered than so far at the LHC) and finally centrality dependence. The production of quark-gluon plasma and its ability to "remember" the initial conditions of the saturated gluonic matter are here of primary interest. Unfortunately RHIC energies are presumably too low for geometrical scaling to work. Nevertheless we show below, that approximate GS can be seen in the RHIC data. To this end we choose the PHOBOS $p_{\rm T}$ distributions measured in gold–gold and copper–copper collisions at 62.4 and 200 GeV per nucleon [23, 24].

Here a new scaling law is particularly interesting. Namely the saturation scale in nucleus–nucleus collisions scales with A as [25] (for review see Ref. [26])

$$Q_{A\,\mathrm{s}}^2 = A^{1/3} Q_{\mathrm{s}}^2 \tag{25}$$

which implies that the relevant scaling variable reads

$$\tau_A = \frac{p_{\mathrm{T}}^2}{A^{1/3} Q_{\mathrm{s}}^2} = \frac{1}{A^{1/3}} \frac{p_{\mathrm{T}}^2}{Q_0^2} \left(\frac{p_{\mathrm{T}}}{W}\right)^{-\lambda} . \tag{26}$$

In Fig. 5 we plot multiplicity distribution for central Au–Au and Cu–Cu collisions in function of p_{T}^2 and τ_A. In this case a slightly higher value of the exponent λ is used, namely $\lambda = 0.3$. We see again that the rescaled spectra seem to fall on one curve, although the alinement of Au and Cu spectra is not perfect for small and medium values of τ_A. Nevertheless a tendency towards geometrical scaling is clearly seen. Similar conclusions can be drawn for more peripheral collisions. A detailed study of the onset of geometrical scaling in heavy ion collisions will be presented elsewhere.

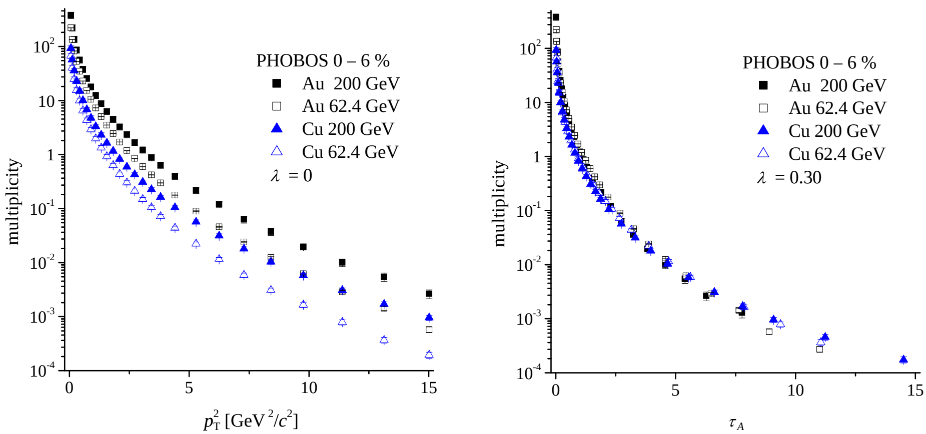

Fig. 5. Multiplicity distribution in heavy ion collisions for Au–Au and Cu–Cu at two RHIC energies 200 and 62.4 GeV [23, 24] plotted in terms of p_{T}^2 (left panel) and scaling variable τ_A (right panel).

5. Conclusions

In this paper we have demonstrated that geometrical scaling originally postulated in deep inelastic scattering [14] is also exhibited by the p_{T} spectra in hadronic collisions [11, 12]. To this end recent CMS data [2] have been analyzed and shown to scale with scaling variable τ defined in Eqs. (20), (21). A simplified model of Gribov, Levin and Ryskin [18] has been used to motivate the appearance of GS in hadronic collisions. This model can be *a priori* used to study the shape of the universal scaling function $F(\tau)$ which deserves a separate study.

A notable difference between DIS and hadronic collisions is that in DIS we deal with totally inclusive cross-section, whereas in pp both hadronization and final state interactions play essential role. Nevertheless, the imprint of the saturation scale $Q_{\rm s}$ is visible in the spectra, which means that the information on the initial fireball survives until final hadrons are formed.

It has been shown that the quality of geometrical scaling is improved if the exponent λ becomes $p_{\rm T}$-dependent [12] in accordance with Q-dependence of $\lambda_{\rm eff}(Q = 2p_{\rm T})$ obtained from DIS. This is a remarkable feature that supports the picture in which medium $p_{\rm T}$ particles are produced from saturated gluonic matter irrespectively of the scattering states.

If so, geometrical scaling should be also present in heavy ion collisions. The detailed studies will be certainly carried out at the LHC. Here we have analyzed PHOBOS data [23, 24] for two RHIC energies and for two different nuclei: gold and copper, and the onset of geometrical scaling has been clearly seen. Interestingly, we have found that the exponent λ that governs geometrical scaling in heavy ion collisions is higher than the one in pp. This is in striking agreement with the fact that multiplicity growth with energy observed by ALICE [4] is faster in heavy ions than in pp. Question arises to what extent the hydrodynamical evolution of the quark-gluon plasma is going to wash out geometrical scaling that is present in the initial state. Further studies should also concentrate on centrality and rapidity dependence of GS.

The author wants to thank Larry McLerran for a number of stimulating discussions that triggered this work and Andrzej Białas for discussion and encouragement. Special thanks are due to Barbara Wosiek for the guidance through the wealth of heavy ion RHIC data. Part of this work has been completed during a short visit at CERN TH Department.

REFERENCES

[1] K. Aamodt *et al.* [ALICE Collaboration], *Eur. Phys. J.* **C65**, 111 (2010); *Eur. Phys. J.* **C68**, 89 (2010); *Eur. Phys. J.* **C68**, 345 (2010); *Phys. Lett.* **B693**, 53 (2010).

[2] V. Khachatryan *et al.* [CMS Collaboration], *J. High Energy Phys.* **1002**, 041 (2010); *Phys. Rev. Lett.* **105**, 022002 (2010); *J. High Energy Phys.* **1101**, 079 (2011).

[3] G. Aad *et al.* [ATLAS Collaboration], *Phys. Lett.* **B688**, 21 (2010); `arXiv:1012.5104 [hep-ex]`.

[4] K. Aamodt *et al.* [ALICE Collaboration], *Phys. Rev. Lett.* **105**, 252301 (2011); *Phys. Rev. Lett.* **106**, 032301 (2011).

[5] L.V. Gribov, E.M. Levin, M.G. Ryskin, *Phys. Rep.* **100**, 1 (1983).

[6] A.H. Mueller, J.W. Qiu, *Nucl. Phys.* **B268**, 427 (1986).

[7] L.D. McLerran, R. Venugopalan, *Phys. Rev.* **49**, 2233 (1994).

[8] L.D. McLerran, R. Venugopalan, *Phys. Rev.* **D49**, 3352 (1994).

[9] L.D. McLerran, R. Venugopalan, *Phys. Rev.* **D50**, 2225 (1994).

[10] A. Ayala, J. Jalilian-Marian, L.D. McLerran, R. Venugopalan, *Phys. Rev.* **D53**, 458 (1996).

[11] L. McLerran, M. Praszalowicz, *Acta Phys. Pol. B* **41**, 1917 (2010); *Acta Phys. Pol. B* **42**, 99 (2011).

[12] M. Praszalowicz, *Phys. Rev. Lett.* **106**, 142002 (2011).

[13] K.J. Golec-Biernat, M. Wusthoff, *Phys. Rev.* **D59**, 014017 (1998); *Phys. Rev.* **D60**, 114023 (1999).

[14] A.M. Stasto, K.J. Golec-Biernat, J. Kwiecinski, *Phys. Rev. Lett.* **86**, 596 (2001).

[15] J. Bartels, K.J. Golec-Biernat, H. Kowalski, *Phys. Rev. D* **66**, 014001 (2002).

[16] C. Adloff *et al.* [H1 Collaboration], *Eur. Phys. J.* **C21**, 33 (2001); S. Chekanov *et al.* [ZEUS Collaboration], *Eur. Phys. J.* **C21**, 443 (2001).

[17] H. Kowalski, L.N. Lipatov, D.A. Ross, G. Watt, *Eur. Phys. J.* **C70**, 983 (2010).

[18] L.V. Gribov, E.M. Levin, M.G. Ryskin, *Phys. Lett.* **B100**, 173 (1981).

[19] J.L. Albacete, C. Marquet, *Phys. Lett.* **B687**, 174 (2010).

[20] E. Levin, A.H. Rezaeian, *Phys. Rev.* **D82**, 014022 (2010); *Phys. Rev.* **D82**, 054003 (2010); `arXiv:1102.2385 [hep-ph]`.

[21] P. Tribedy, R. Venugopalan, *Nucl. Phys.* **A850**, 136 (2011); `arXiv:1101.5922 [hep-ph]`.

[22] D. Kharzeev, E. Levin, *Phys. Lett.* **B523**, 79 (2001).

[23] B.B. Back *et al.* [PHOBOS Collaboration], *Phys. Rev. Lett.* **94**, 082304 (2005).

[24] B. Alver *et al.* [PHOBOS Collaboration], *Phys. Rev. Lett.* **96**, 212301 (2006).

[25] D. Kharzeev, M. Nardi, *Phys. Lett.* **B507**, 121 (2001).

[26] L. McLerran, *Acta Phys. Pol. B* **41**, 2799 (2010).